Effect Of Chemical Reaction On Nanofluid Flow Over An Unsteady Stretching Sheet In Presence Of Heat Source

[1*]Pradyumna kumar Pattnaik, [2]Niranjan Mishra, [3] Madan MohanModuly,
[4]Niladri Bhusan Mohapatra
[1,2,3]Department of Mathematics, College of Engg. and Technology, Bhubaneswar, 751029
[4]Department of Mechanical Engg.,Indus College of Engg. and Technology, Bhubaneswar, 752050
[1]Email: pattnaikphd@gmail.com

Abstract

An investigation has been made for the effect of chemical reaction of an unsteady boundary layer flow of a nanofluid over a heated stretching sheet with heat source/sink, magnetic and porosity parameter. The unsteadiness in the flow field is caused by the time-dependence of the stretching velocity, free stream velocity and the surface temperature. The unsteady boundary layer equations are transformed to a system of non-linear ordinary differential equations and solved numerically using a shooting method together with Runge–Kutta 4th order scheme. For supporting the results and discussion part some graphs are included.

Keywords: *Nanofluid, Heat and mass transfer, Stretching sheet, Chemical reaction, Magnetic and Porosity parameter.*

1. Introduction:

Nanofluid is a fluid suspension containing metallic or non-metallic nanoparticles with a typical size of (1- 100 nm) dispersed into the base fluid. The concept of nanofluids was first introduced by Choi, [1] where he proposed the suspension of nanoparticles in a base fluid such as water, oil, and ethylene glycol. Nano fluid is an environmental friendly and also provides better efficiency than the fluids using currently. Nano fluid is a colloidal mixture of nano sized particles in a base fluid to enhance the heat transfer characteristics suited for practical application. However, existence of solid particles leads to interesting characteristics in the fundamental thermo-physical properties nanofluids. Thermal conductivity, viscosity, density and stability have been investigated throughout the recent years by

Nomenclature

u, v	velocity along x-,y-axis	x, y	horizontal and vertical axis
t	time	U_e	ambient velocity along y-axis
ν_f	kinematic viscosity of the base fluid	σ	electrical conductivity
B_0	applied magnetic field	ρ_f	density of the base fluid
k_p^*	porosity parameter	T	temperature of the fluid
α	thermal diffusivity of the base fluid	D_B	Brownian diffusion coefficient
C	nanoparticle volume fraction	D_T	thermophoretic diffusion coeff.
T_∞	free stream value of temperature	q_r	radiative heat flux in the $y-$axis
$(\rho c_p)_f$	specific heat parameters of the base fluid	q_0	heat source parameter
k_c^*	chemical reaction parameter	τ	ratio of heat capacities
$(\rho c_p)_s$	specific heat parameters of the nanoparticle	$\sigma *$	Stefan–Boltzmann constant
$k*$	mean absorption coefficient	U_w	stretching velocity
T_w	temperature of the sheet	C_w	nanoparticle volume fraction
a	stretching rate	b	strength of the stagnation flow
λ	buoyancy force	η	similarity variable
ψ	stream function	f	non-dimensional velocity
θ	non-dimensional temperature	ϕ	non-dimensional concentration
S	unsteadiness parameter	β	stretching parameter
M	magnetic parameter	K_p	porosity parameter
$\mathrm{P_r}$	Prandtl number	N_r	thermal radiation parameter
N_b	Brownian motion number	N_t	thermophoresis number
H	heat source parameter	L_e	Lewis number
K_c	non-dimensional chemical reaction parameter	κ	thermal conductivity
C_f	skin friction coefficient	N_u	local Nusselt number
S_h	local Sherwood number	C_{fr}	reduced skin friction coefficient
N_{ur}	reduced Nusselt number	**Subscripts**	
S_{hr}	reduced Sherwood number	w	condition at wall
Re_x	local Reynolds number	∞	condition at free stream

many researchers. Density of fluid is an important thermo-physical property. Like viscosity, density of any fluid also has direct impact over pressure drop and pumping power and it also affects on Reynolds number, Nusselt number, thermal diffusivity as well as heat transfer coefficient of a heat transfer fluid. However, only a limited number of studies have been conducted on density of nanofluids [2,3]. Buongiorno [4] attempted to explain the increase in the thermal conductivity of such fluids and developed a model that took into account the particle Brownian motion and thermophoresis. It is a new class of heat transfer fluids due to its attractive enhancements on thermo-physical properties and heat transfer. For heating and cooling process, cooling is an essential part of multitudinous industrial and civil application such as power generation, chemical process, microelectronics, transportation, air condition and microsized application etc. [5,6]. Makinde [7] has investigated the Sakiadis flow of nano fluids with viscous dissipation and Newtonian heating. Motsumi and Makinde [8] studied the effects of thermal radiation and viscous dissipation on boundary layer flow of nanofluids over a permeable moving flat plate. Nadeem et.al. [9] investigated the Non-orthogonal stagnation point flow of a nano non-Newtonian fluid towards a stretching surface with heat transfer. Das[10] investigated the Lie group analysis of stagnation-point flow of a nanofluid. Das[11] also investigated the Nanofluid flow over a shrinking sheet with surface slip. Nadeem et al.[12] studied the heat transfer analysis of water-based nanofluid over an exponentially stretching sheet. Kunetsov and Neild [13] revised a model to investigate the natural convective boundary layer flow of a nano fluid past a vertical plate. Nadeem et al. [14] studied the MHD three-dimensional boundary layer flow of casson nano fluid past a linearly stretching sheet with convective boundary condition. Pattnaik and Biswal [15, 16] have studied the MHD free convective boundary layer flow over a vertical surface through porous media. Mishra et. al [17] studied the analysis of heat and mass transfer with MHD and chemical reaction effects on viscoelastic fluid over a stretching sheet. Mishra et. al [18] investigated the effect of heat source and double stratification on MHD free convection in a micropolar fluid.

Moreover, the present study is an extension of the work of Das et. al [19] including Magnetic parameter, porosity parameter, heat source and chemical reaction parameter, which they have not considered.

2. Mathematical formulation

The study of two-dimensional unsteady boundary layer flow of a nanofluid over a heated stretching sheet with chemical reaction in presence of magnetic and porosity parameter and heat source/sink has been considered. The coordinate system under consideration is such that x measures the distance along the sheet and y measures the distance normally into the fluid (Fig. 1). The flow is assumed to be confined to $y > 0$. Two equal and opposite forces are impulsively applied along the x – axis so that the sheet is stretched keeping to fixed origin. Let us consider that for time $t < 0$ the fluid and heat flows are steady. The unsteady fluid and heat flows start at $t=0,$ the sheet being stretched with the velocity $U_w\left(x,\ t\right)$ along the x-axis. It is also assumed that the ambient fluid is moved with a velocity $U_e\left(x,\ t\right)$ in the $y-$direction toward the stagnation point on the plate. The temperature of the sheet $T_w\left(x,\ t\right)$ and the value of nanoparticle volume fraction $C_w\left(x,\ t\right)$ at the surface vary both with the distance x along the sheet and time t and higher than the ambient temperature T_∞ and concentration C_∞ respectively. In view of thermal equilibrium, there is no slip between the base fluid and suspended nanoparticles. Since the velocity of the nanofluid is low (laminar flow), the viscous dissipative heat is assumed to be negligible here. An external variable magnetic field B_0 is applied along the positive y-direction. Magnetic field is sufficiently weak to ignore magnetic induction effects. The physical properties of the fluid are assumed to be uniform, isotropic, and constant.

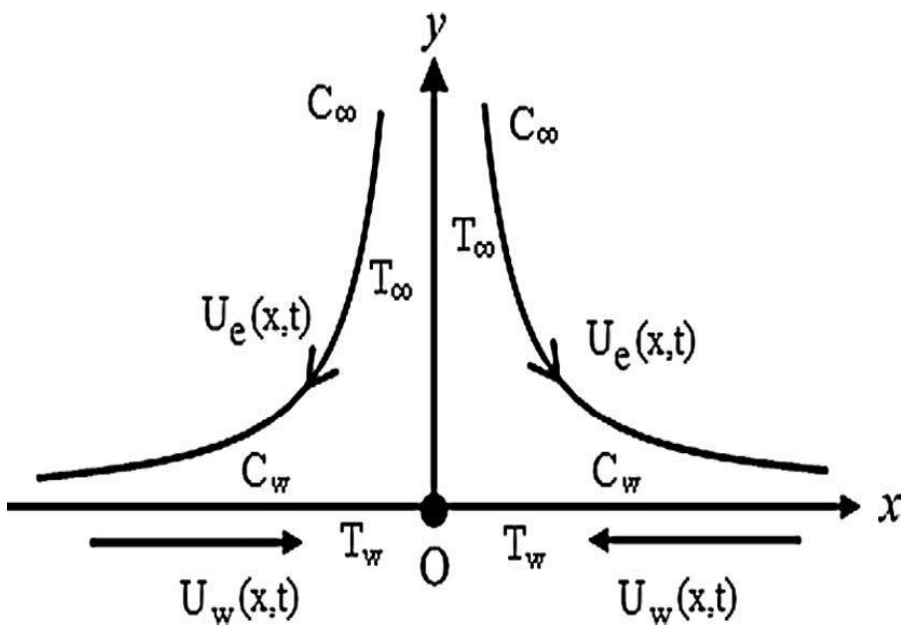

Fig.(1) Physical Model

The governing equations of the flow in two dimensions are as follows:

$$\frac{\partial u}{\partial x}+\frac{\partial v}{\partial y}=0 \tag{1}$$

$$\frac{\partial u}{\partial t}+u\frac{\partial u}{\partial x}+v\frac{\partial u}{\partial y}=\frac{\partial U_e}{\partial t}+U_e\frac{\partial U_e}{\partial x}+\nu_f\frac{\partial^2 u}{\partial y^2}-\left(\frac{\sigma B_0^2}{\rho_f}+\frac{\nu_f}{k_p^*}\right)(u-U_e) \tag{2}$$

$$\frac{\partial T}{\partial t}+u\frac{\partial T}{\partial x}+v\frac{\partial T}{\partial y}=\alpha\frac{\partial^2 T}{\partial y^2}+\tau\left[D_B\frac{\partial C}{\partial y}\frac{\partial T}{\partial y}+\left(\frac{D_T}{T_\infty}\right)\left(\frac{\partial T}{\partial y}\right)^2\right]-\frac{1}{(\rho c_p)_f}\frac{\partial q_r}{\partial y}+\frac{q_0}{(\rho c_p)_f}(T-T_\infty) \quad (3)$$

$$\frac{\partial C}{\partial t}+u\frac{\partial C}{\partial x}+v\frac{\partial C}{\partial y}=D_B\frac{\partial^2 C}{\partial y^2}+\left(\frac{D_T}{T_\infty}\right)\frac{\partial^2 T}{\partial y^2}-k_c^{*}(C-C_\infty) \quad (4)$$

$$\alpha=\frac{\kappa}{(\rho c_p)_f}\text{ and }\tau=\frac{(\rho c_p)_s}{(\rho c_p)_f}.$$

Using the Rosseland approximation, the radiative heat flux is given by (Brewster [20])

$$q_r=-\frac{4\sigma^*}{3k^*}\frac{\partial T^4}{\partial y} \quad (5)$$

where $T^4=4T_\infty^3T-3T_\infty^4$ (6)

So from equation (5),

$$\frac{\partial q_r}{\partial y}=-\frac{16T_\infty^3\sigma^*}{3k^*}\frac{\partial^2 T}{\partial y^2} \quad (7)$$

Putting equation (7) in equation (3) we have,

$$\frac{\partial T}{\partial t}+u\frac{\partial T}{\partial x}+v\frac{\partial T}{\partial y}=\alpha\left(1+\frac{16T_\infty^3\sigma^*}{3k^*\kappa}\right)\frac{\partial^2 T}{\partial y^2}+\tau\left[D_B\frac{\partial C}{\partial y}\frac{\partial T}{\partial y}+\left(\frac{D_T}{T_\infty}\right)\left(\frac{\partial T}{\partial y}\right)^2\right]+\frac{q_0}{(\rho c_p)_f}(T-T_\infty) \quad (8)$$

The boundary conditions for the problem are as follows:

$$\left.\begin{array}{ll} u=U_w(x,t),\ v=0, T=T_w(x,t), C=C_w(x,t) & \text{at } y=0 \\ u\to U_e(x,t), T\to T_\infty, C\to C_\infty & \text{as } y\to\infty \end{array}\right\} \quad (9)$$

Here the stretching and free stream velocities are of the form:

$$U_w=\frac{ax}{1-\lambda t} \quad (10)$$

$$U_e=\frac{bx}{1-\lambda t} \quad (11)$$

where $a,b,\lambda(>0)$ constants having dimension $(time)^{-1}$ with $(\lambda t<1,\lambda\geq 0)$.

The wall temperature and nanoparticle volume fraction are given by,

$$T_w\left(x,\ t\right)=T_\infty+T_0\left[\frac{ax^2}{2v_f}\right](1-\lambda t)^{-2} \quad (12)$$

$$C_w\left(x,\ t\right)=C_\infty+C_0\left[\frac{ax^2}{2v_f}\right](1-\lambda t)^{-2} \quad (13)$$

where T_0 and C_0 are positive reference temperature and nanoparticle volume fraction respectively such that $0 \le T_0 \le T_w$ and $0 \le C_0 \le C_w$. Note that the above expressions are valid for time $t < \lambda^{-1}$.

3. Non-dimensionalization

Introducing the following similarity variable and dimensionless functions:

$$\left.\begin{array}{l} \eta = \left(\dfrac{a}{\nu_f(1-\lambda t)}\right)^{\frac{1}{2}} y, \qquad \psi = \left(\dfrac{a\nu_f}{(1-\lambda t)}\right)^{\frac{1}{2}} x\, f(\eta), \\ T = T_\infty + \left[\dfrac{ax^2}{(1-\lambda t)^2}\right]\theta(\eta), C = C_\infty + \left[\dfrac{ax^2}{(1-\lambda t)^2}\right]\phi(\eta) \end{array}\right\} \tag{14}$$

where the stream function (ψ) is defined as:

$u = \dfrac{\partial \psi}{\partial y}$ and $v = -\dfrac{\partial \psi}{\partial x}$.

Putting the above values in equation (1), we get,

$$u = \left(\frac{ax}{(1-\lambda t)}\right) f'(\eta), \quad v = -\left(\frac{a\nu_f}{(1-\lambda t)}\right)^{\frac{1}{2}} f'(\eta) \tag{15}$$

Now substituting Eq. (14) into Eqs. (2), (4) and (8), the following ordinary differential equations are obtained as follows:

$$f''' + f''\left(f - \frac{1}{2}\eta S\right) - f'(f'+S) + \beta^2 + \beta S - \left(M + \frac{1}{K_p}\right)(f'-\beta) = 0 \tag{16}$$

$$\frac{1}{P_r}(1+N_r)\theta'' - S(2\theta + \frac{1}{2}\eta\theta') + f\theta' - (2f'+H)\theta + N_b\theta'\phi' + N_t\theta'^2 = 0 \tag{17}$$

$$\frac{1}{\mathrm{P_r}\, L_e}\phi'' - S(2\phi + \frac{1}{2}\eta\phi') + f\phi' - (2f'+K_c)\phi + \frac{N_t}{\mathrm{P_r}\, L_e N_b}\theta'' = 0 \tag{18}$$

The boundary conditions (9) take the form

$$\begin{array}{l} f'(0) = 1,\ f(0) = 0,\ \theta(0) = 1, \phi(0) = 1, \\ f'(\infty) \to \beta, \quad \theta(\infty) \to 0, \quad \phi(\infty) \to 0 \end{array} \tag{19}$$

where

$$\left.\begin{array}{l} S = \dfrac{\lambda}{a}, \beta = \dfrac{b}{a}, \mathrm{P_r} = \dfrac{\nu_f}{\alpha_f}, N_r = \dfrac{16T_\infty^3\sigma^*}{3k^*\kappa}, N_b = \dfrac{\tau D_B(C_w - C_\infty)}{\nu_f}, N_t = \dfrac{\tau D_T(T_w - T_\infty)}{\nu_f T_\infty} \\ L_e = \dfrac{\alpha_f}{D_B},\ H = \dfrac{q_0(1-\lambda t)}{a(\rho c_p)_f},\ M = \dfrac{\sigma B_0^2(1-\lambda t)}{a\rho},\ K_p = \dfrac{ak_p^*}{\nu(1-\lambda t)},\ K_c = \dfrac{k_c^*(1-\lambda t)}{a} \end{array}\right]$$

4. Physical quantities

The skin friction coefficient, local Nusselt number and local Sherwood number are respectively defined as:

$$C_f = \frac{\mu}{\rho_f U_w^2}\left(\frac{\partial u}{\partial y}\right)_{y=0} \tag{20}$$

$$N_u = \frac{x}{\kappa(T_w - T_\infty)}\left[\kappa\left(\frac{\partial T}{\partial y}\right)_{y=0} - \frac{4\sigma *}{3k *}\left(\frac{\partial T^4}{\partial y}\right)_{y=0}\right] \tag{21}$$

$$S_h = \frac{x}{(T_w - T_\infty)}\left(\frac{\partial C}{\partial y}\right)_{y=0} \tag{22}$$

Substituting equation (14) into equations (20)-(22), we get, the reduced skin friction coefficient, reduced Nusselt number and reduced Sherwood number as:

$$C_{fr} = \sqrt{\mathrm{Re}_x}C_f = f''(0) \tag{23}$$

$$N_{ur} = \sqrt{\mathrm{Re}_x}N_u = -(1+N_r)\theta'(0) \tag{24}$$

$$S_{hr} = \sqrt{\mathrm{Re}_x}S_h = -\phi'(0) \tag{25}$$

where $\mathrm{Re}_x = \frac{U_w x}{v_f}$ is the local Reynolds number.

5. Method of solution

The set of non-linear coupled differential Eqs. (16)–(18) with appropriate boundary conditions given in Eq. (19) constitute a two-point boundary value problem. The equations are highly non-linear and so, cannot be solved analytically. Therefore, these equations are solved numerically by using Runge–Kutta fourth order with shooting technique. The asymptotic boundary conditions in (19) at $\eta \to \infty$ are replaced by those at $\eta = \eta_\infty$ as is usually the standard practice in the boundary layer analysis. The inner iteration is counted until the nonlinear solution converges with a convergence criterion of 10^{-6} in all cases.

6. Results and discussion

In this paper, the effects of chemical reaction on an unsteady boundary layer flow of a nanofluid over a heated stretching sheet with heat source/sink, magnetic and porosity parameter have been investigated. Numerical computations for velocity, temperature and concentration are obtained by using Runge–Kutta fourth order with shooting technique. In order to analyze the results, numerical computation has been carried out (using the method described in the previous section), for various values of the unsteadiness (S) ,magnetic (M) ,porosity (K_p) ,thermophoretic (N_t) , Brownian motion (N_b) ,heat source (H) and chemical reaction (K_c) parameter with Prandtl number (P_r) and Lewis number (Le) .In the simulation the default values of the parameters are considered as $S = 0.4,\ N_b = 0.1, N_t = 0.1,\ P_r = 0.71,\quad N_r = 0.2, \beta = 0.5, M = 1, K_p = 0.5, H = 1$ and $K_c = 2$ unless otherwise specified. For the shake of validity, fig.2 is represented. It is clear that velocity profile increases for increasing values of stretching parameter (β).Fig.3 represents the variations of velocity profiles due to magnetic parameter (M) in presence $(K_p = 0.5)$ /absence $(K_p = 100)$ of porosity parameter. It is marked that velocity profile decreases with an increment of magnetic parameter both presence/absence of porosity parameter. It is observed that presence of magnetic field produces Lorentz force which resists the motion of the fluid both in absence/presence of porous matrix. Figs. (4-6) represent the variations of velocity, temperature and concentration profiles due to unsteady parameter (S) both in presence $(K_p = 0.5)$ /absence $(K_p = 100)$ of porosity parameter. It is marked that all the profiles decrease with an increment of (S) both in presence/absence of porosity parameter. Velocity profile decreases due to the presence of buoyancy force acting on velocity profile. It is noteworthy that both temperature and nanoparticle volume fraction (concentration) profiles satisfy the far field boundary conditions asymptotically, thus supporting the validity of the numerical results obtained. It is noticed that by escalating S, both temperature and concentration boundary layer thickness decreases with increase in the values of S near the boundary layer region in the presence of thermal radiation and satisfies the far field boundary conditions asymptotically. Fig.(7,8) represents the variation in both temperature and concentration profiles due to increasing values of thermal radiation parameter (N_r) for the case of steady flow $(S = 0)$ and unsteady flow $(S = 0.5)$. It is observed that the fluid temperature increases as N_r increases due to the fact that the conduction effect of the nanofluid increases in the presence of thermal radiation. Therefore higher values of radiation parameter imply higher surface heat flux and so, increase the temperature within the boundary layer region. It is also observed that thermal boundary layer thickness increases with increasing the values of N_r for both steady and unsteady cases. The impact of thermal radiation parameter N_r on the nanoparticles volume fraction profiles is presented in Fig. 8. It can easily be seen from figure that the nanoparticle volume fraction decreases near the boundary surface. It should be noted that the effect is prominent for unsteady flow than that of steady flow. Figs. (9, 10) represent the variations in both temperature and concentration profile for increased values of Brownian motion parameter (N_b) both for the case of steady and unsteady cases. It is clear that the fluid temperature is found to increase with the increasing values of N_b for both $(S=0)$ and $(S=0.5)$. This is due to the fact that the increased Brownian motion increases the thickness of thermal boundary layer, which ultimately enhances the temperature. The nanoparticle volume fraction distribution is presented in Fig. 10 for various values of Brownian motion parameter (N_b) when for steady flow $(S=0)$ and for unsteady flow $(S=0.5)$. The curves show that the nanoparticle volume fraction decreases with increasing N_b near the boundary layer region for both steady and unsteady flows. Figs. (11, 12) represents the variation of fluid temperature and nanoparticle volume fraction (concentration) profiles for different values of thermophoretic parameter (N_t) both in steady and unsteady cases. It has been observed that fluid temperature increases on increasing values of N_t in the boundary layer region and, as a consequence, thickness of the thermal boundary layer increases. This enhancement is due to the nanoparticle of high thermal conductivity being driven away from the hot sheet to the quiescent nanofluid. It is seen from Fig. 12 that the thermophoretic parameter N_t produces an increase in the nanoparticle volume fraction for both the steady and unsteady cases. It is interesting to note from the figure that distinctive peaks in the profiles occur in region adjacent to the wall for higher values of thermophoretic parameter N_t. This means that the nanoparticle volume fraction near the sheet is higher than the nanoparticle volume fraction at the sheet and consequently, and nanoparticles are expected to transfer to the sheet due to the thermophoretic effect. Figs. (13, 14) represents the variation of fluid temperature and nanoparticle volume fraction (concentration) profiles for different values of Prandtl number (P_r) both in steady $(S=0)$ and unsteady $(S=0.5)$ cases. High Prandtl number causes low thermal diffusivity. As a result, the temperature profile becomes thinner and thinner at thermal boundary layer for both steady and unsteady cases. It is interesting to note that temperature profile also gets thinner near the boundary layer when value of unsteady parameter increases. But the reverse effect has been observed in the variation of nanoparticle volume fraction and it gets accelerated in absence of unsteady parameter $(S = 0)$. It is interesting to note that concentration profile jumps to its maximum peak near the boundary for steady case. This has been clearly observed in fig. 14. Figs. (15, 16) represents the variation of fluid temperature and nanoparticle volume fraction (concentration) profiles for different values of heat source (H) both in steady $(S = 0)$ and unsteady $(S = 0.5)$ cases. Temperature profile gets decelerated for increasing values of heat source parameter H for both in steady and unsteady cases. But it attains its maximum value in steady state case. It has also been observed that for an increment of unsteady parameter, temperature profile gets decelerated. But the reverse effect has been observed for nanoparticle volume fraction for both steady and unsteady cases. Fig. 17 exhibits the nanoparticle volume fraction profiles for several values of Lewis number L_e for both steady and unsteady flows. It is seen that the nanoparticle volume fraction decreases with increasing values of L_e and this implies an accompanying reduction in the thickness of the concentration boundary layer thickness. Also the nanoparticle volume fraction profiles decrease asymptotically to zero at the edge of the boundary layer. Fig. 18 exhibits the effect of chemical reaction parameter (K_c) on nanoparticle volume fraction profiles for both steady and unsteady flows. Chemical reaction parameter shows a retarding effect on concentration distribution as the reaction proceeds with increased values of K_c. Fig. 19 exhibits the effect of magnetic parameter (M) on temperature profiles for both steady and unsteady flows. It has been observed that temperature gets enhanced for increment of magnetic parameter both in presence/absence of porous matrix. This is due to the resistive force, Lorentz force, which retards the velocity profiles and action temperature gets accelerated. Fig. 20 exhibits the effect of stretching parameter (β) on temperature profiles for both steady and unsteady flows. It has been observed that temperature gets decelerated for increment of stretching parameter both in steady and unsteady flows.

7. Conclusions

_ Magnetic parameter decreases the fluid velocity both in presence/absence of porous matrix whereas reverse effect occurred in temperature cases.

_ Stretching parameter increases the fluid velocity both in steady and unsteady cases whereas reverse effect occurred in temperature cases.

_ Heat source decreases the fluid temperature but enhances nanoparticle volume fraction both in presence/absence of porous matrix.

_ Chemical reaction decreases the nanoparticle volume fraction both in presence/absence of porous matrix.

_ Increasing the Brownian motion parameter, Lewis number and unsteadiness parameter lead to reduce the nanoparticle volume fraction near the boundary layer region but the effect is reverse for the thermophoretic parameter.

_ The fluid temperature and the thermal boundary layer thickness increase for increasing thermal radiation, Brownian motion and thermophoresis whereas the effect is opposite for unsteadiness parameter.

_ It is seen that the reduced Skin Friction coefficient increases for increasing values of stretching parameter for both steady and unsteady cases where as for magnetic parameter in presence/absence of porosity parameter, reverse trend is observed.

_ It is seen that the reduced Nusselt number increases as the Brownian motion parameter, Lewis number, Prandtl number, heat source parameter, unsteadiness parameter and thermal radiation parameter increase whereas the opposite trend is noticed in the case of thermophoretic parameter, magnetic and porosity parameter.

_ It is seen that the reduced Sherwood number decreases as the Brownian motion parameter, Lewis number, Prandtl number, heat source parameter, unsteadiness parameter, thermal radiation parameter thermophoretic parameter, magnetic and porosity parameter increase.

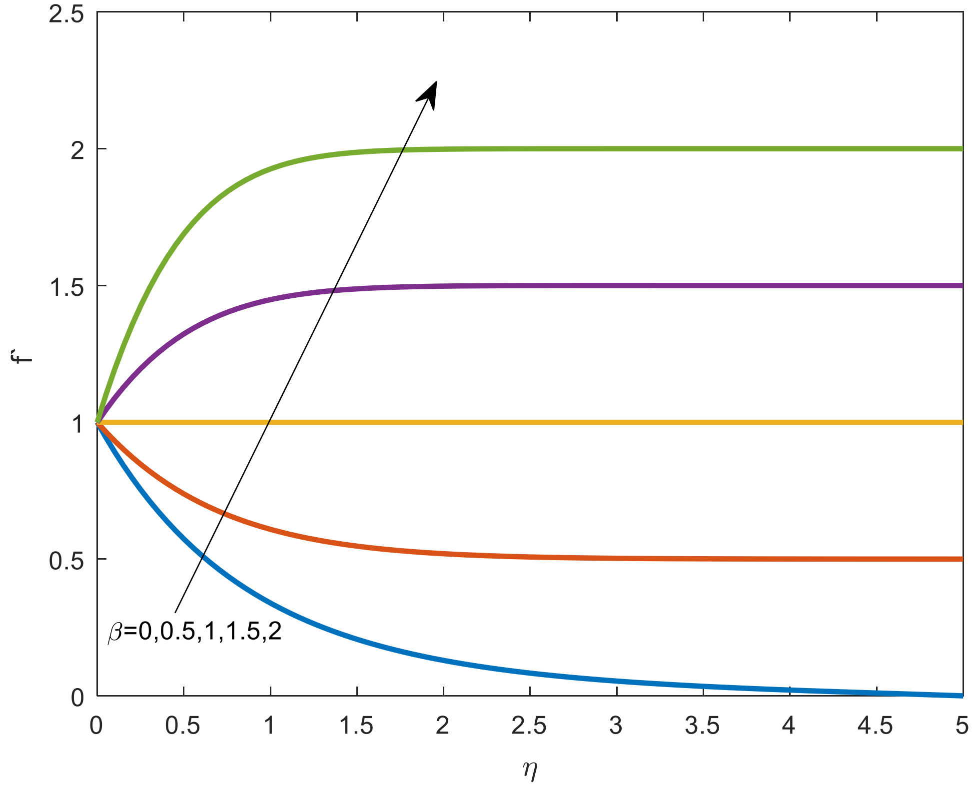

Fig.2 Velocity profile for various values of β

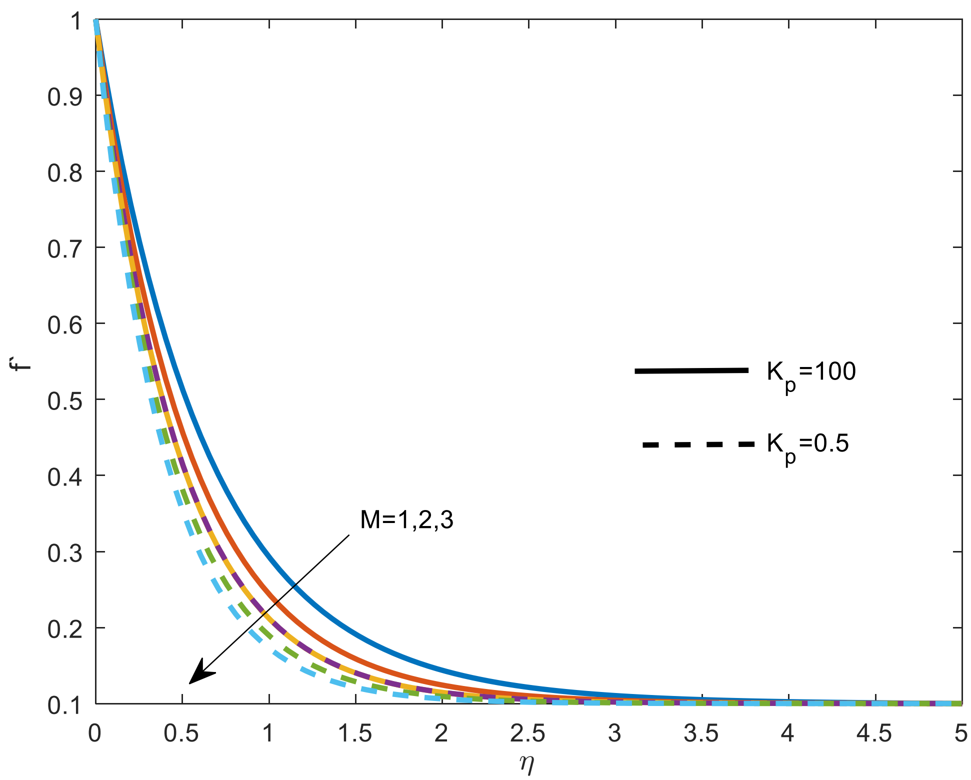

Fig. 3 Velocity profiles for various values of M and K_p

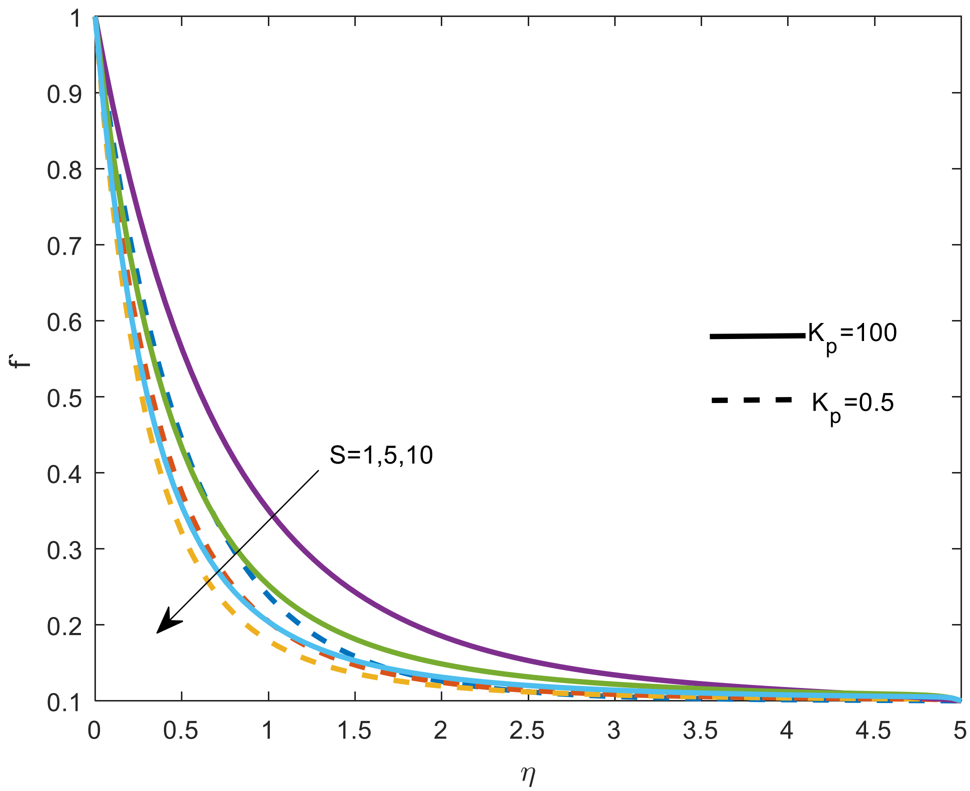

Fig. 4 Velocity profiles for various values of S and K_p

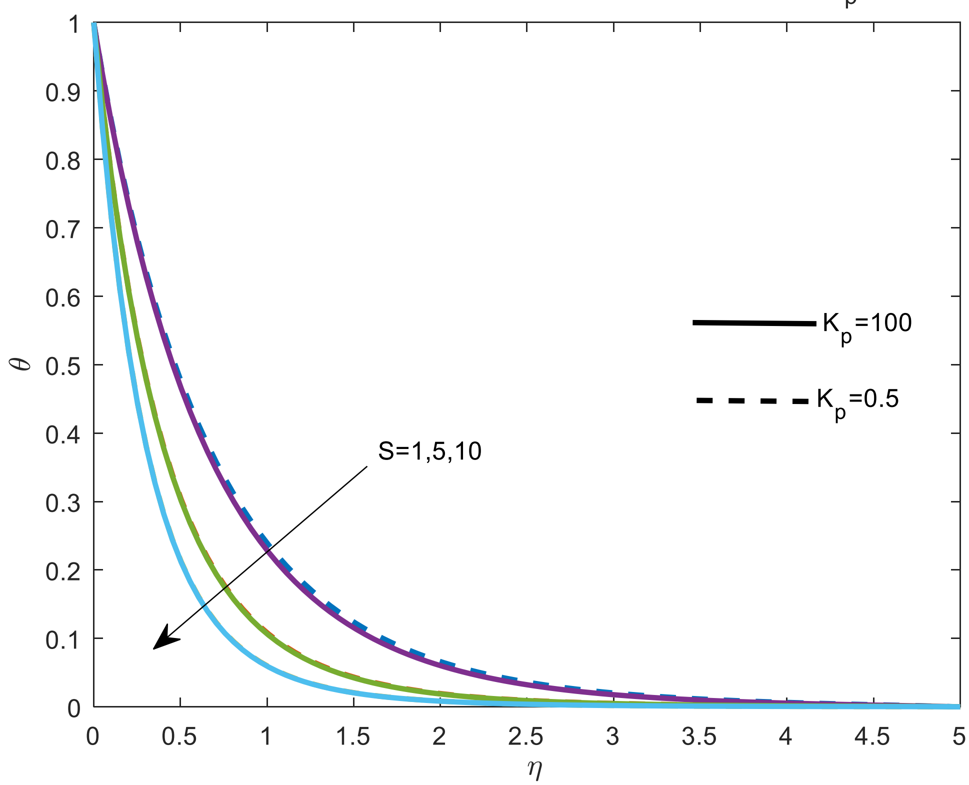

Fig. 5 Temperature profile for various values of S and K_p

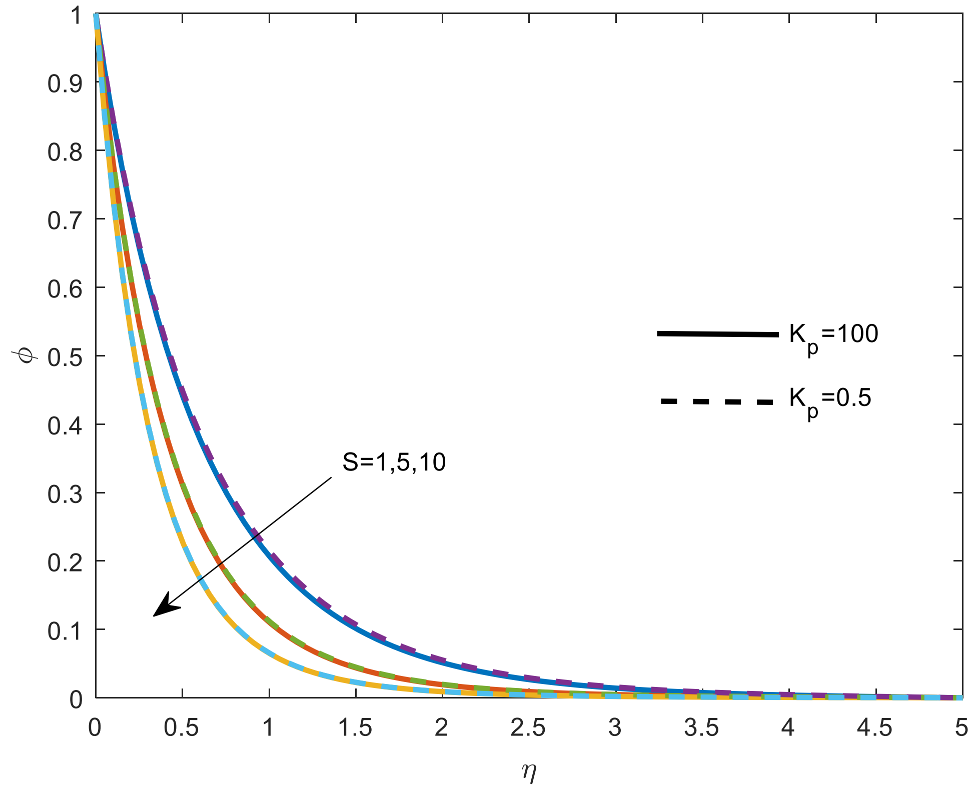

Fig. 6 Concentration profiles for various values of S and K_p

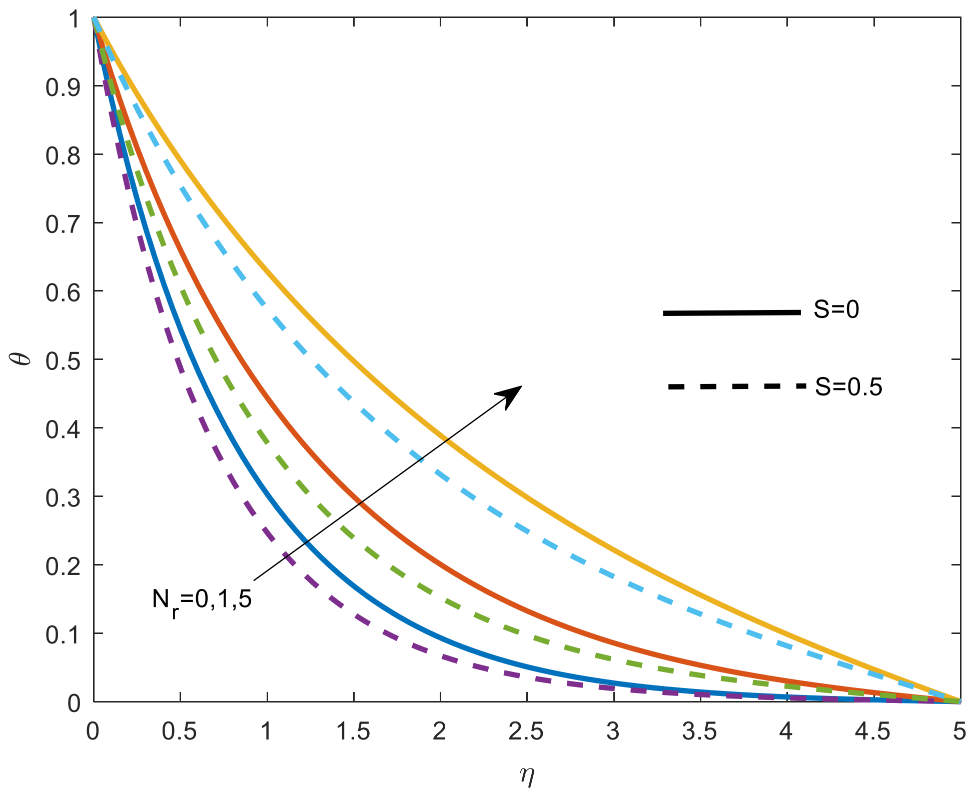

Fig. 7 Temperature profiles for various values of N_r and S

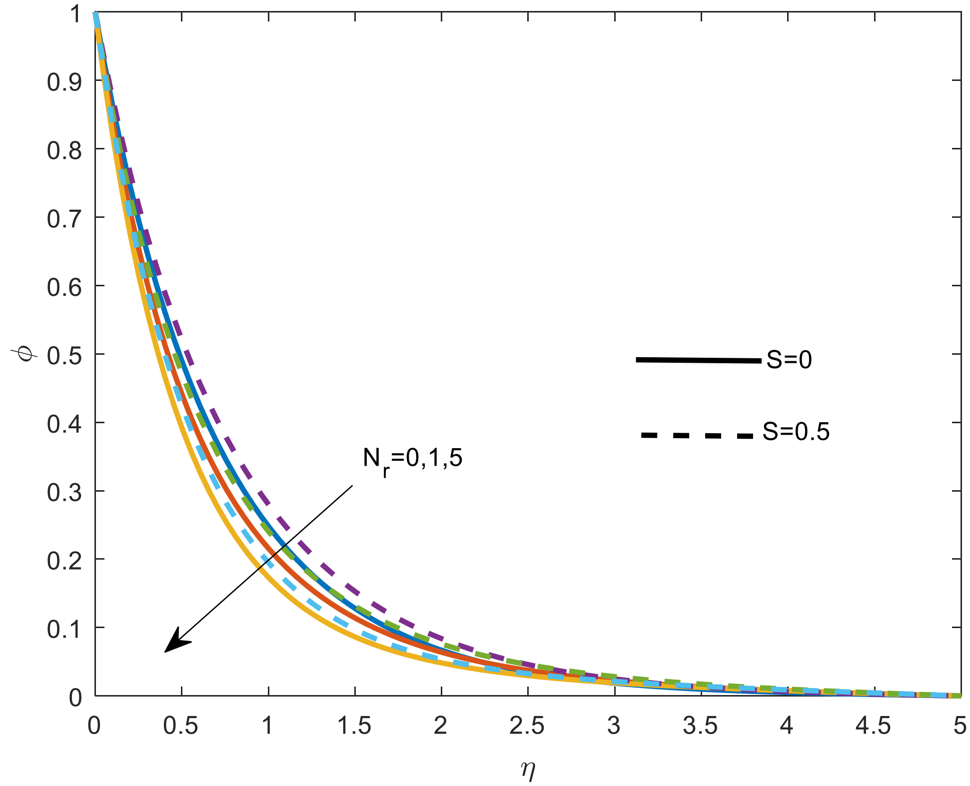

Fig. 8 Concentration profiles for various values of N_r and S

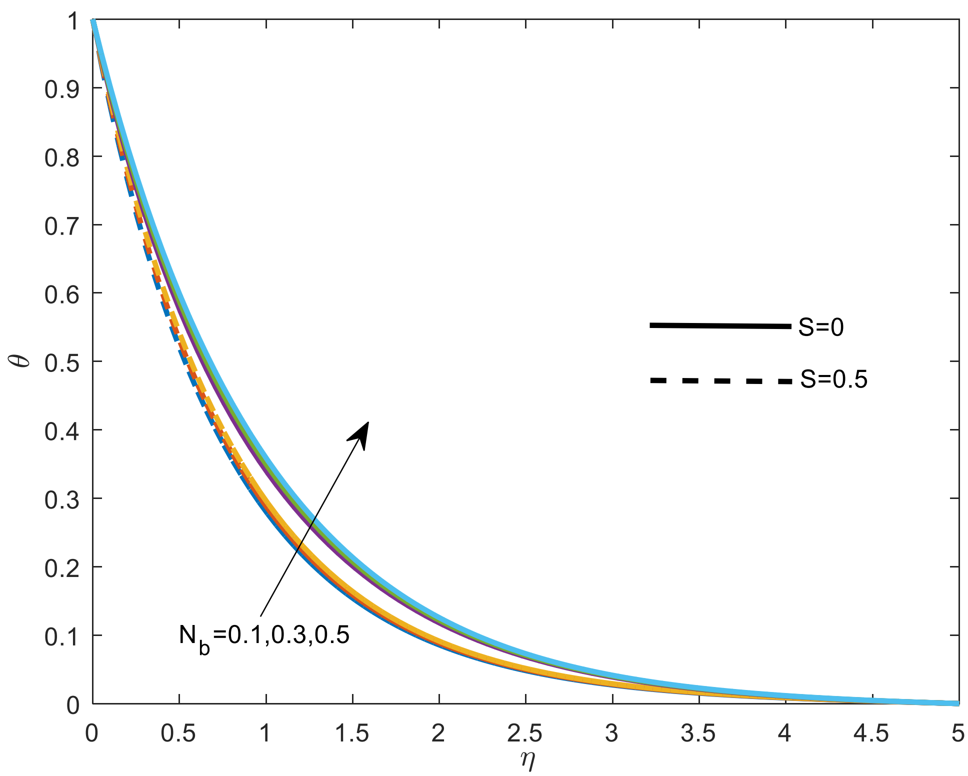

Fig. 9 Temperature profiles for various values of N_b and S

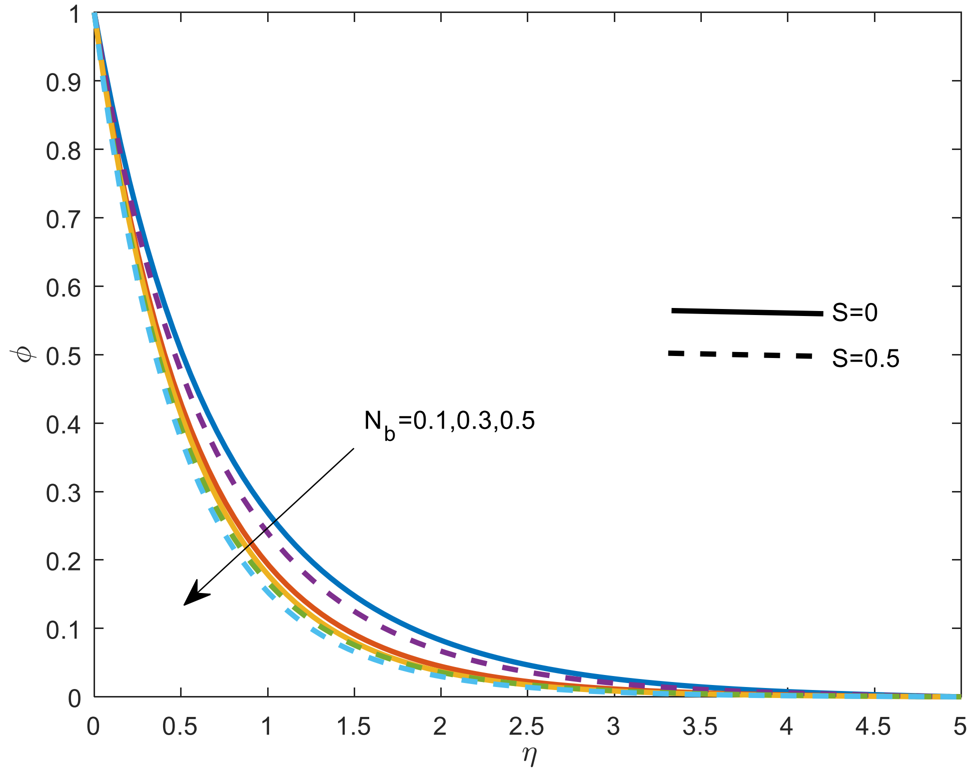

Fig. 10 Concentration profiles for various values of N_b and S

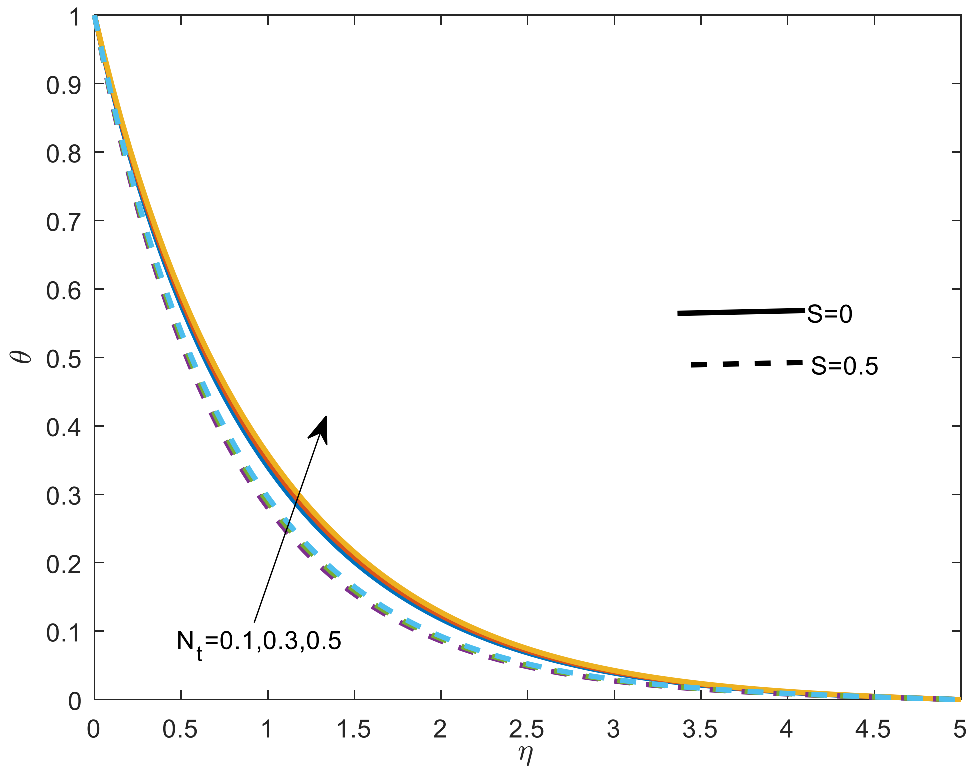

Fig. 11 Temperature profiles for various values of N_t and S

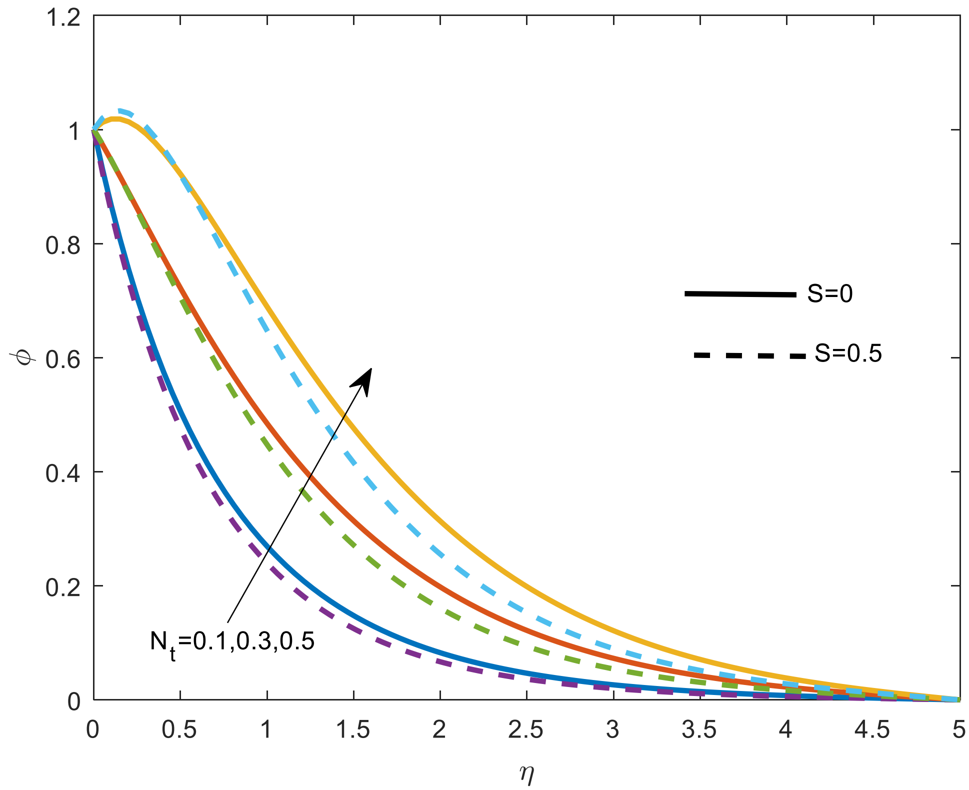

Fig. 12 Concentration profile for various values of N_t and S

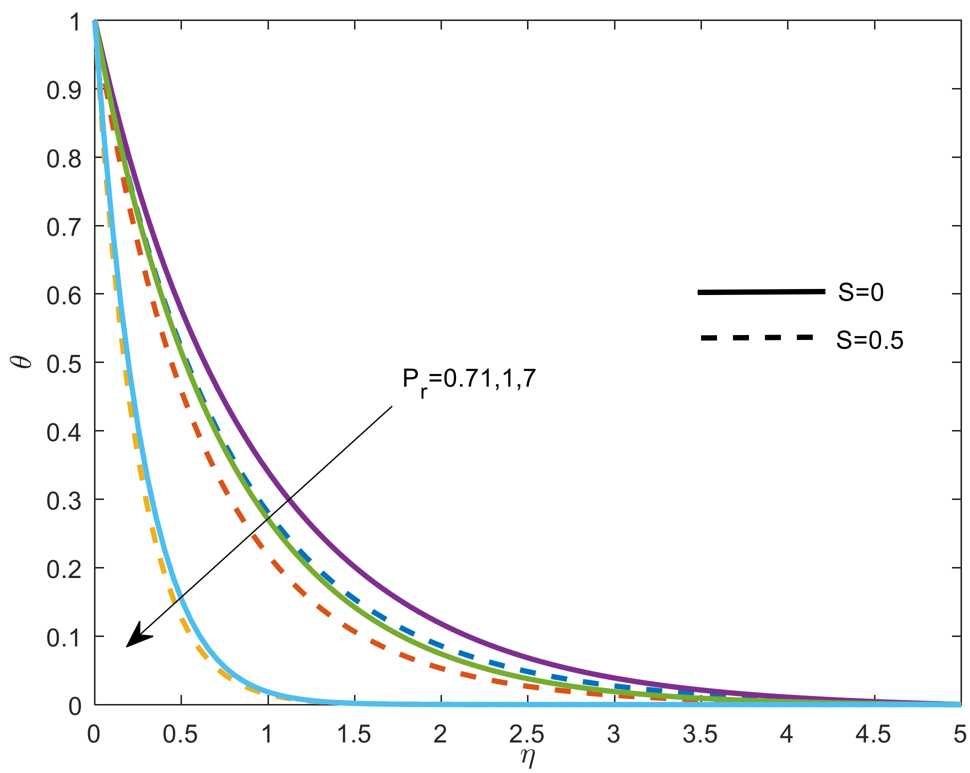

Fig.13 Temperature profiles for various values of P_r and S

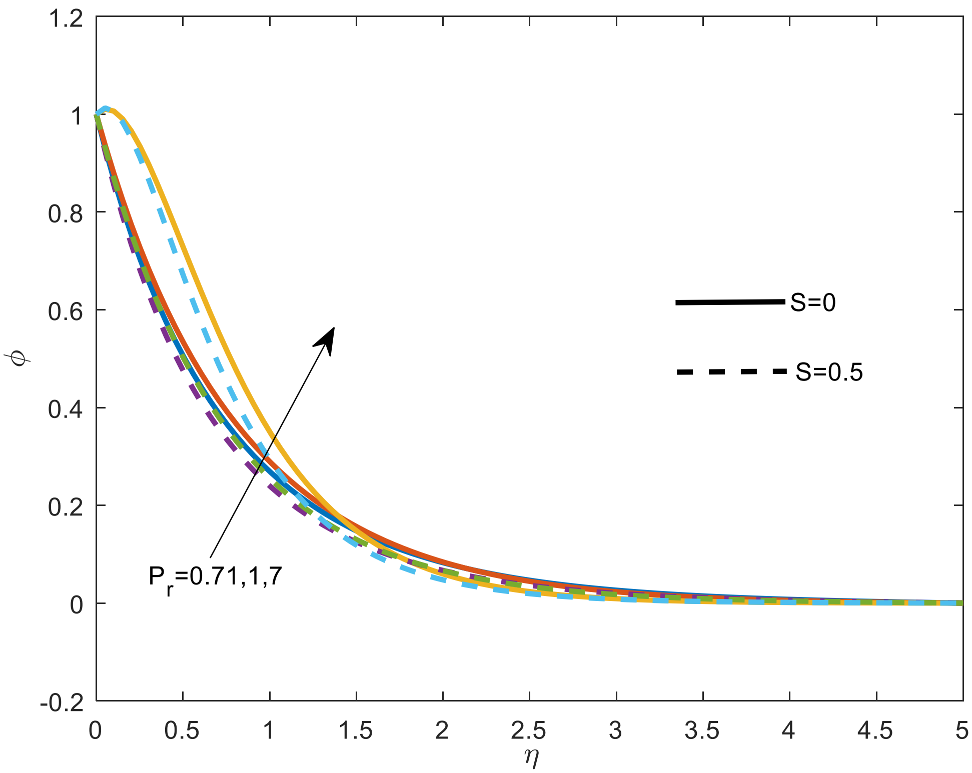

Fig.14 Concentration profiles for various values of P_r and S

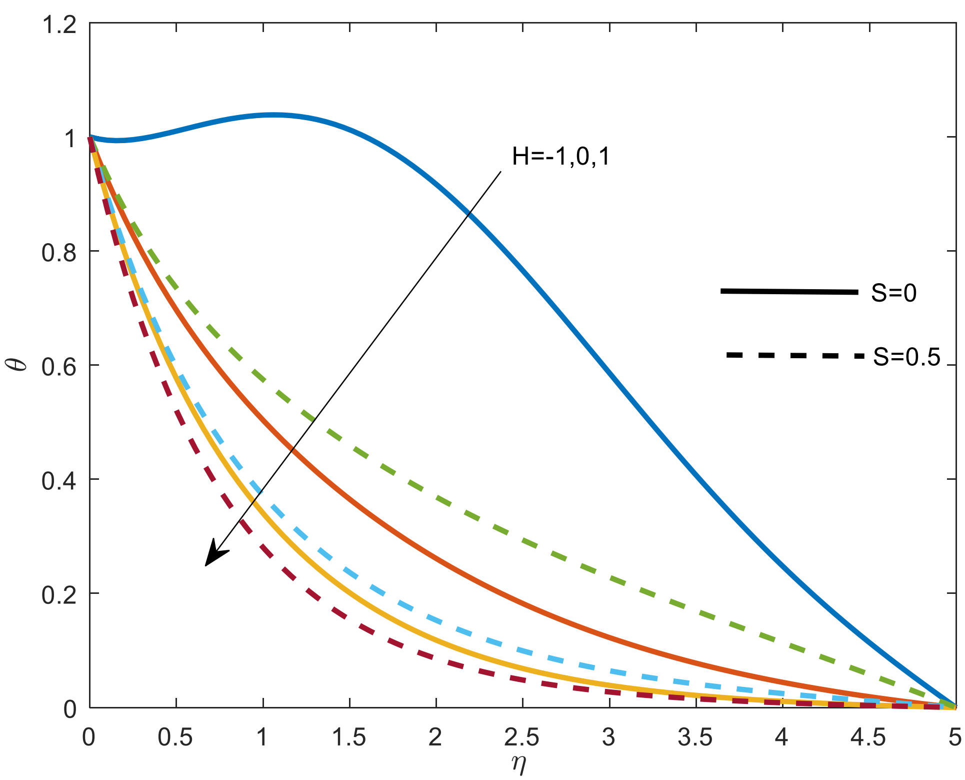

Fig. 15 Temperature profiles for various values of H and S

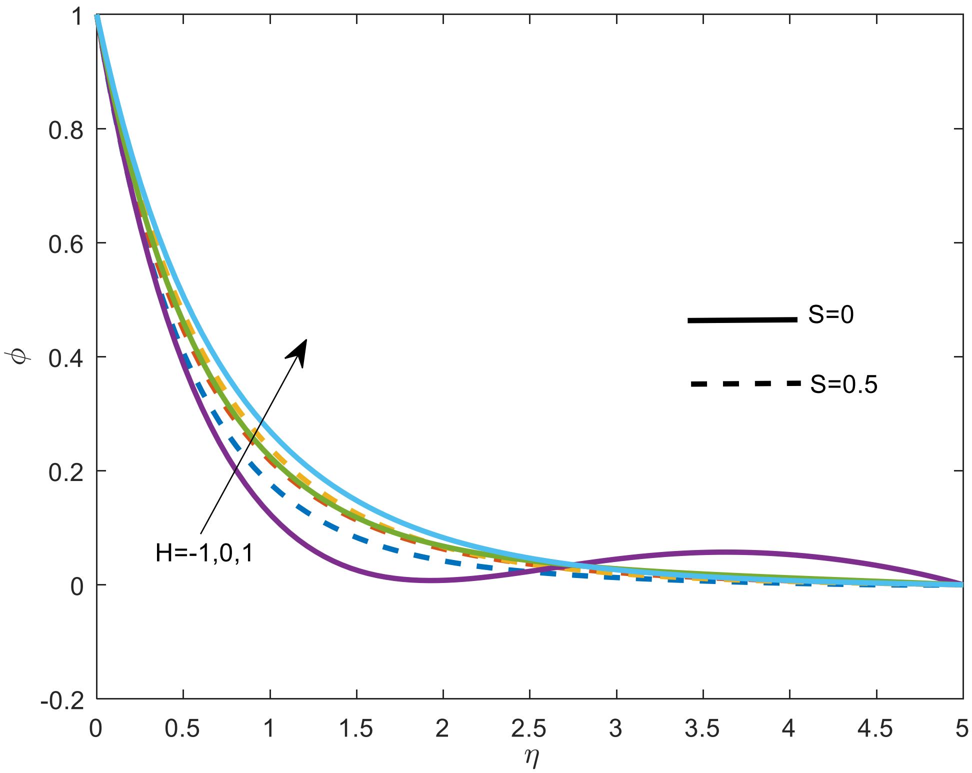

Fig. 16 Concentration profiles for various values of H and S

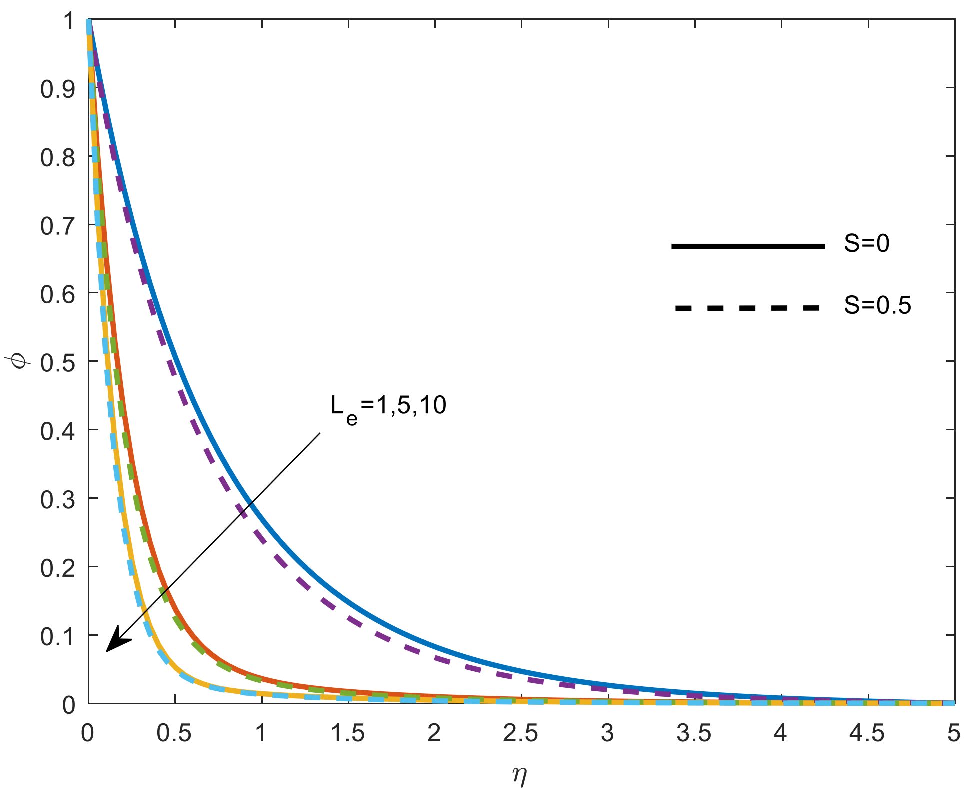

Fig. 17 Concentration profiles for various values of L_e and S

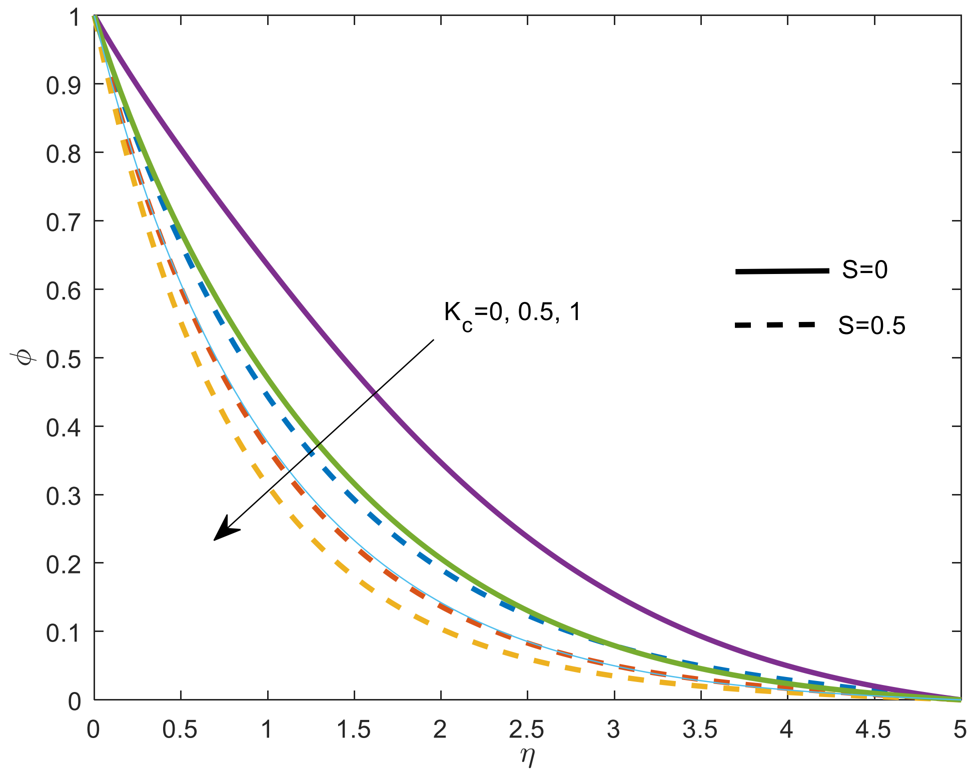

Fig. 18 Concentration profiles for various values of K_c and S

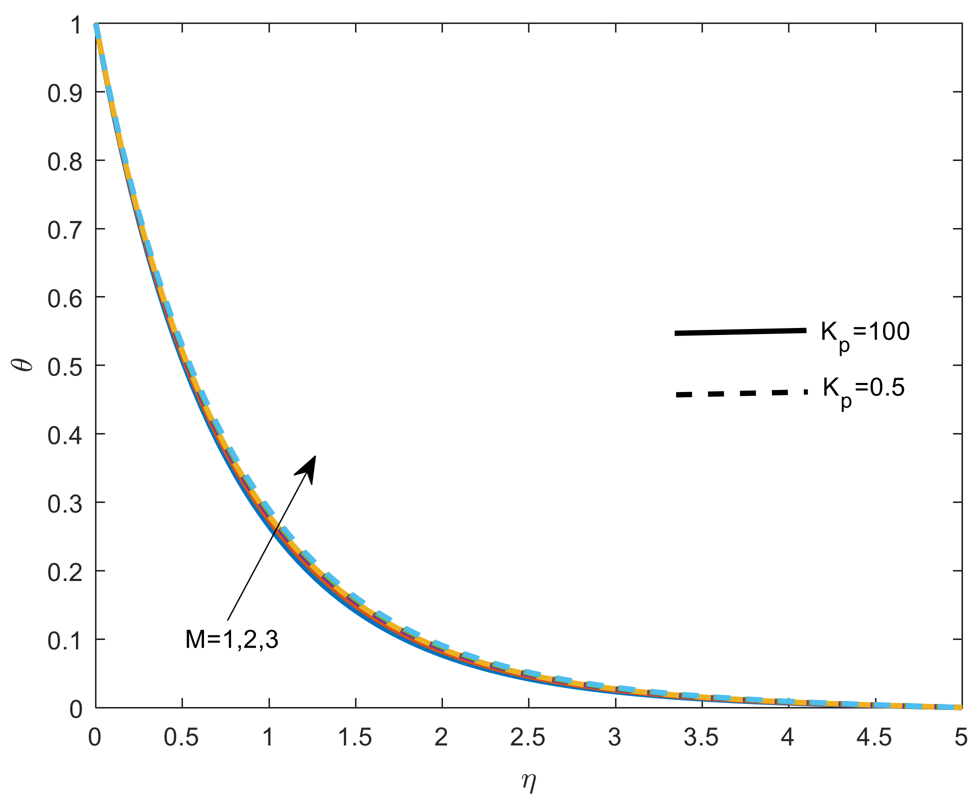

Fig.19 Temperature profile for various values of M and K_p

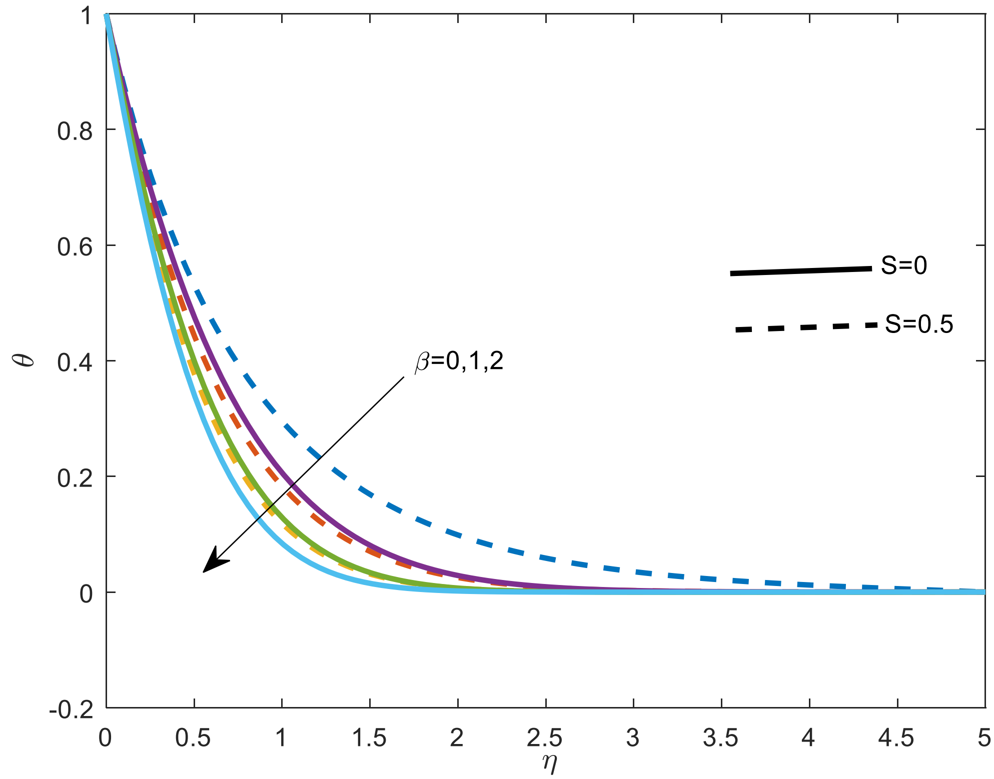

Fig. 20 Temperature profile for various values of β and S

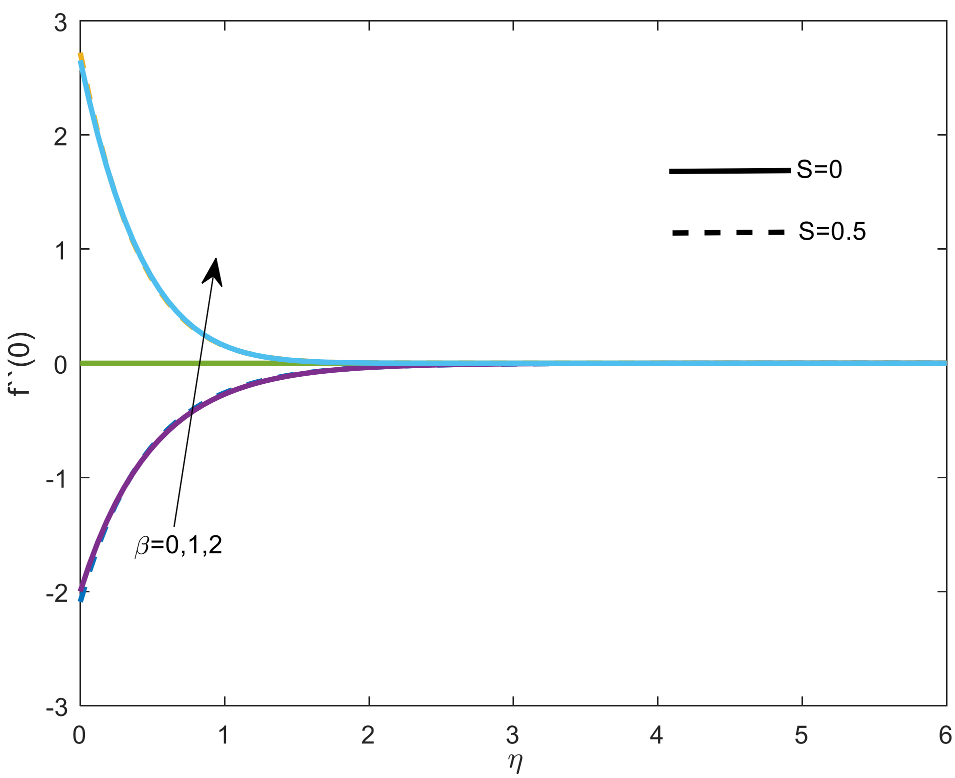

Fig. 21 Reduced skin friction coefficient for various values of β

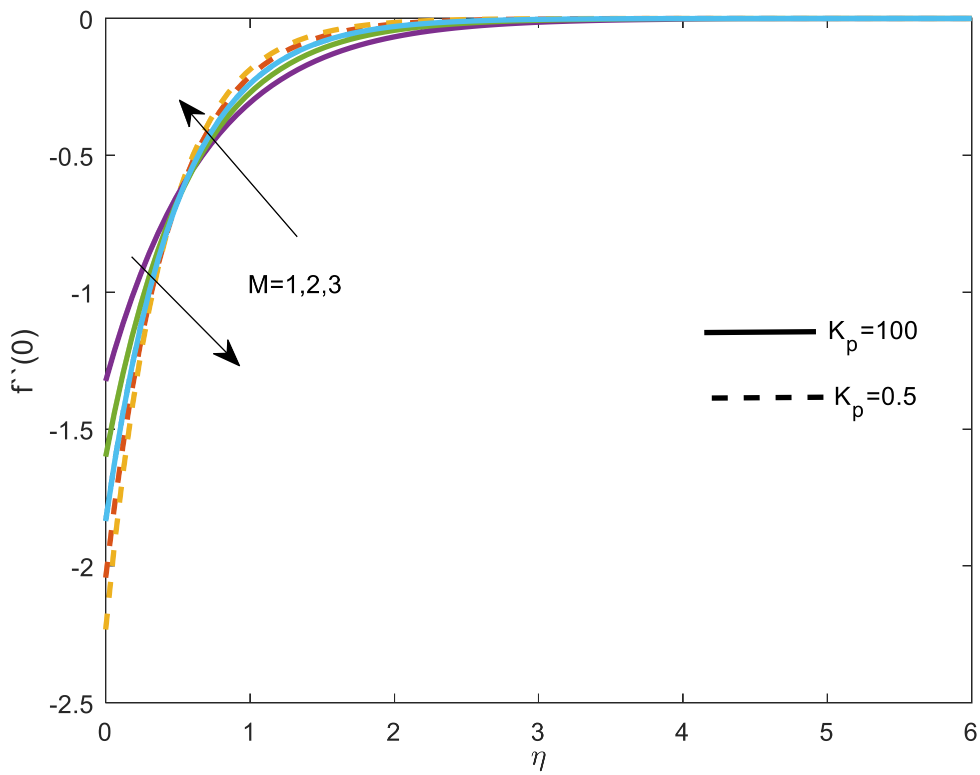

Fig. 22 Reduced skin friction coefficient for various values of M and K_p

Fig. 23 Reduced Nusselt Number N_{ur}

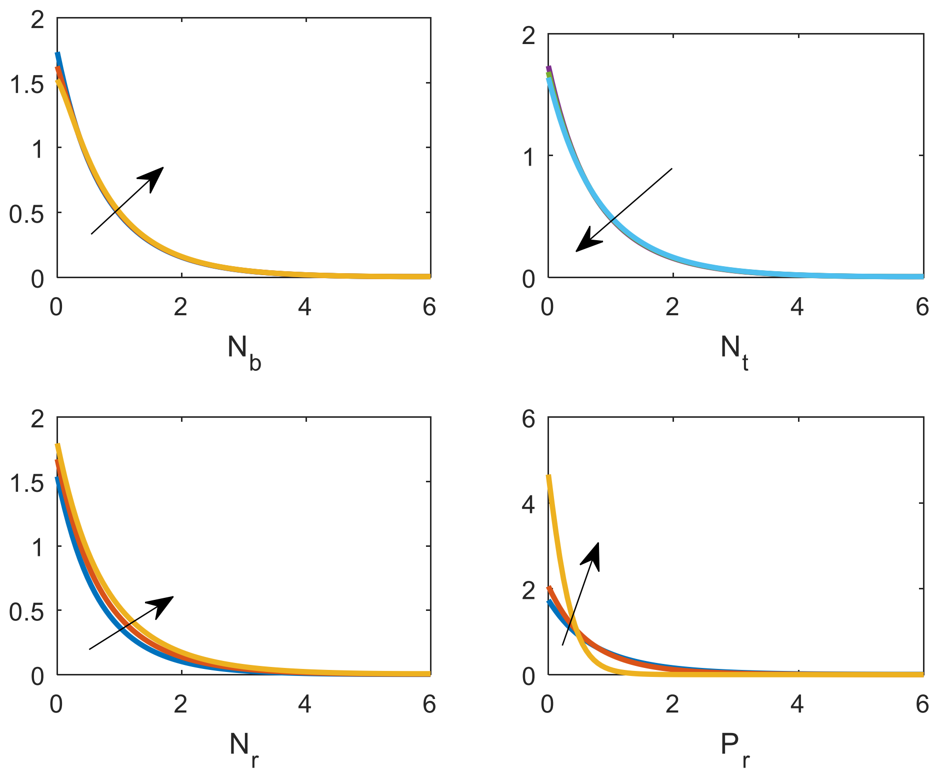

Fig. 24 Reduced Nusselt Number N_{ur}

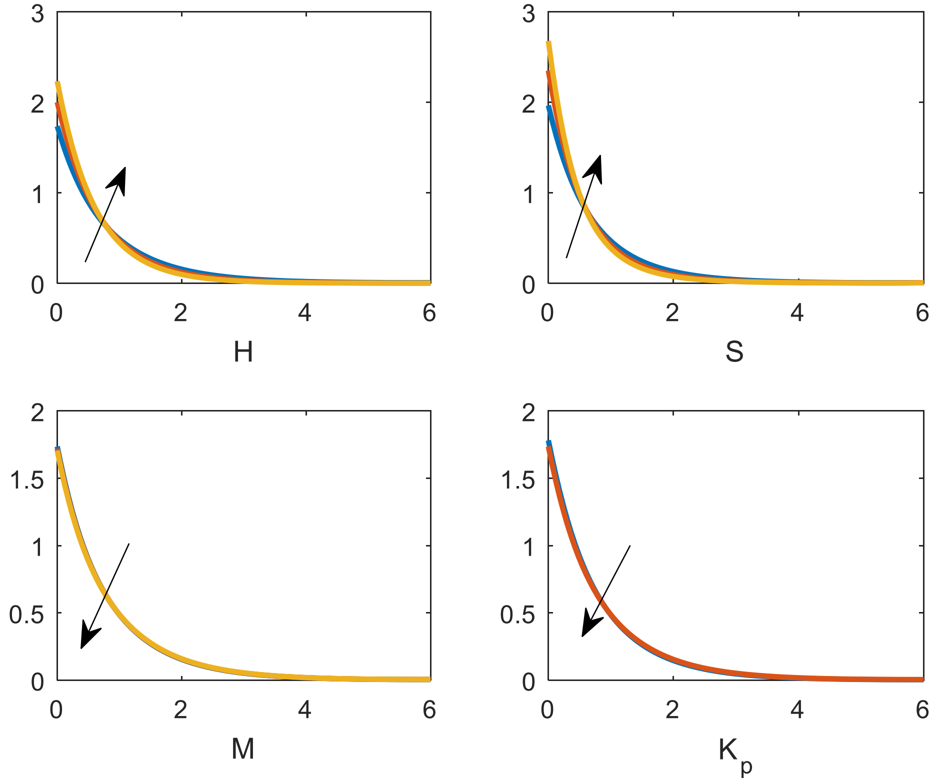

Fig. 25 Reduced Sherwood Number S_{hr}

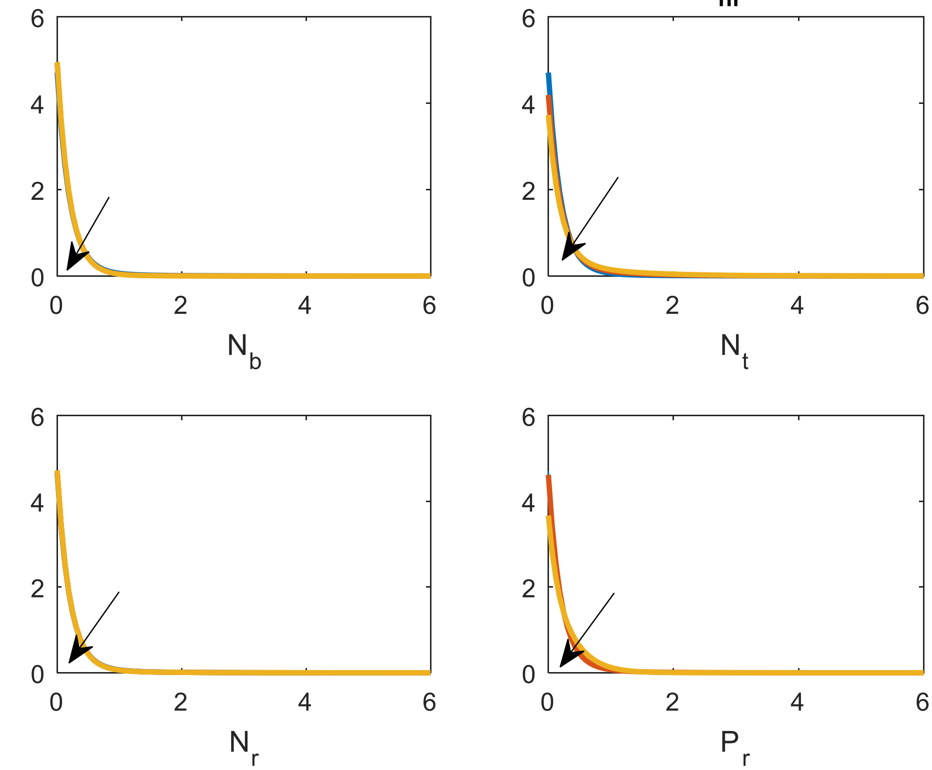

Fig. 26 Reduced Sherwood Number S_{hr}

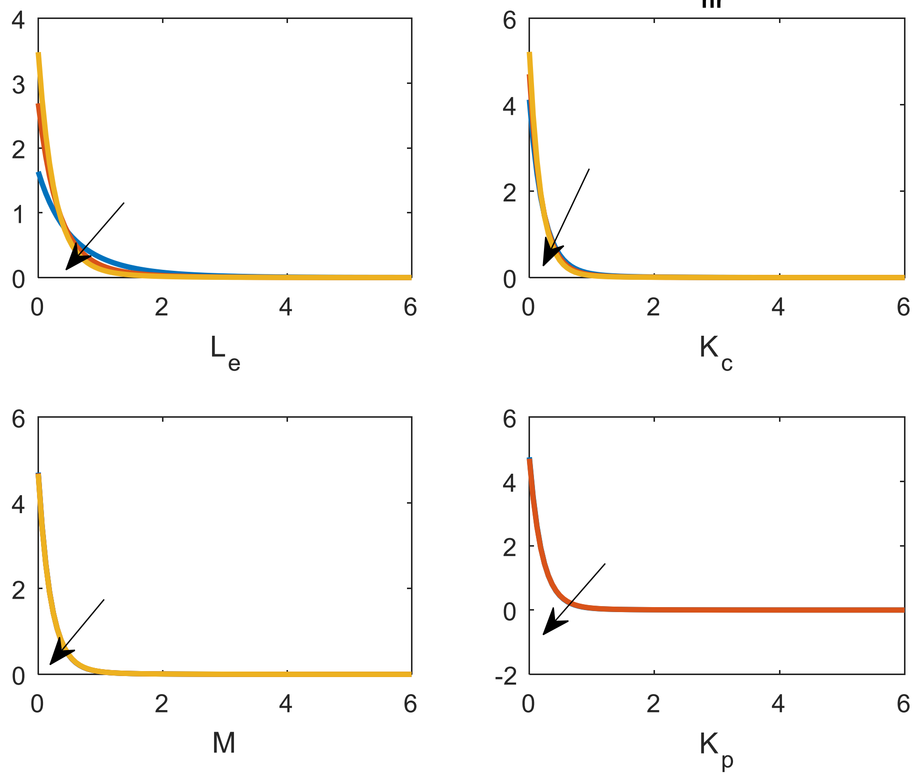

References:

[1] *S.U.S. Choi, Enhancing thermal conductivity of fluids with nanoparticles, ASME Fluids Eng. Div. 231(1995) 99–105.*

[2] *Lee S, Choi S U S, Li S, Eastman J,J. Heat Trans.(1999)121- 280.*

[3] *Chandrasekar M and Suresh S, Heat Trans. Eng. 30(2009)1136.*

[4] *J. Buongiorno, Convective transport in nano fluids, ASME J. Heat Transfer, 128(2006)240-250.*

[5] *Nuntaphan A, Vithayasai S, Vorayos N, Vorayos N and Kiatsiriroat, T Int. Comm. Heat Mass Tran. 37 (2010) 287.*

[6] *Saidur R, Leong K Y, Mohammad H A, Renew. Sustain. Energy Rev. 15(2011)1646.*

[7] *O.D. Makinde, Analysis of Sakiadis flow of nano fluids with viscous dissipation and Newtonian heating, Appl. Math.Mech.33(12)(2012)1545-1554(English Edition).*

[8] *T.G. Motsumi,O.D. Makinde,Effects of thermal radiation and viscous dissipation on boundary layer flow of nanofluids over a permeable moving flat plate, Phys. Scr.86(2012),045003(8pp).*

[9] *S. Nadeem, R. Mehmood, N.S. Akbar, Non-orthogonal stagnation point flow of a nano non-Newtonian fluid towards a stretching surface with heat transfer, Int. J. Heat Mass Transfer 57 (2013) 679-689.*

[10] *K. Das, Lie group analysis of stagnation-point flow of a nanofluid, Microfluidics Nanofluidics 15(2013)267–274.*

[11] *K. Das, Nanofluid flow over a shrinking sheet with surface slip, Microfluidics Nanofluidics 16 (2014) 391–401.*

[12] *S. Nadeem, R.U. Haq, Z.H. Khan, Heat transfer analysis of water-based nanofluid over an exponentially stretching sheet, Alexandria Eng. J. 53 (1) (2014) 219–224.*

[13] *A. V. Kunetsov, D.A. Neild, Natural convective boundary layer flow of a nano fluid past a vertical plate : a revised model, Int. J. Ther. Sci. 77(2014) 126-129.*

[14] *S. Nadeem, R. U. Haq, N.S. Akbar, MHD three-dimensional boundary layer flow of casson nano fluid past a linearly stretching sheet with convective boundary condition, IEEE. Trans. Nanotech.13 (2014) 109-115.*

[15] *P. K. Pattnaik and T. Biswal ,MHD free convective boundary layer flow of a viscous fluid at a vertical surface through porous media with non-uniform heat source,IJISET,2(3)(2015).*

[16] *Pattnaik P K, Biswal T, Analytical Solution of MHD Free Convective Flow through Porous Media with Time Dependent Temperature and Concentration, Walailak J Sci & Tech, 12 (9) (2015) 749-762.*

[17] *Mishra S R, Pattnaik P K, Bhatti M M, Abbas T, Analysis of heat and mass transfer with MHD and chemical reaction effects on viscoelastic fluid over a stretching sheet, Indian J Phys(2017), DOI 10.1007/s12648-017-1022-2.*

[18] *Mishra S R, Pattnaik P K, Dash G C, Effect of heat source and double stratification on MHD free convection in a micropolar fluid, Alexandria Engineering Journal, 54 (2015) 681–689.*

[19] *K. Das, P.R. Duari , P. K. Kundu , Nanofluid flow over an unsteady stretching surface in presence of thermal radiation,Alexandria Engineering Journal,53,(2014)737-745.*

[20] *M.Q. Brewster, Thermal Radiative Transfer Properties, Wiley, New York, (1972).*